

# RFold: Towards Simple yet Effective RNA Secondary Structure Prediction

Cheng Tan <sup>\*1 2</sup> Zhangyang Gao <sup>\*1 2</sup> Stan Z. Li <sup>2</sup>

## Abstract

The secondary structure of ribonucleic acid (RNA) is more stable and accessible in the cell than its tertiary structure, making it essential in functional prediction. Though deep learning has shown promising results in this field, current methods suffer from either the post-processing step with a poor generalization or the pre-processing step with high complexity. In this work, we present RFold, a simple yet effective RNA secondary structure prediction in an end-to-end manner. RFold introduces novel Row-Col Softmax and Row-Col Argmax functions to replace the complicated post-processing step while the output is guaranteed to be valid. Moreover, RFold adopts attention maps as informative representations instead of designing hand-crafted features in the pre-processing step. Extensive experiments demonstrate that RFold achieves competitive performance and about eight times faster inference efficiency than the state-of-the-art method. The code and Colab demo are available in [github.com/A4Bio/RFold](https://github.com/A4Bio/RFold).

## 1. Introduction

Ribonucleic acid is essential in structural biology for its diverse functional classes (Crick, 1970; Noller, 1984; Rich & RajBhandary, 1976; Geisler & Coller, 2013). The functions of an RNA molecule are determined by its structure (Sloma & Mathews, 2016). The secondary structure, which contains the nucleotide base pairing information, as shown in Fig. 1, is vital for the correct functions of RNA molecules (Fox & Woese, 1975; Fallmann et al., 2017; Westhof & Fritsch, 2000). Although experimental assays such as X-ray crystallography (Cheong et al., 2004), nuclear magnetic resonance (NMR) (Fürtgig et al., 2003), and cryogenic electron microscopy (Fica & Nagai, 2017) can be implemented to

determine RNA secondary structure, they suffer from low throughput and expensive cost.

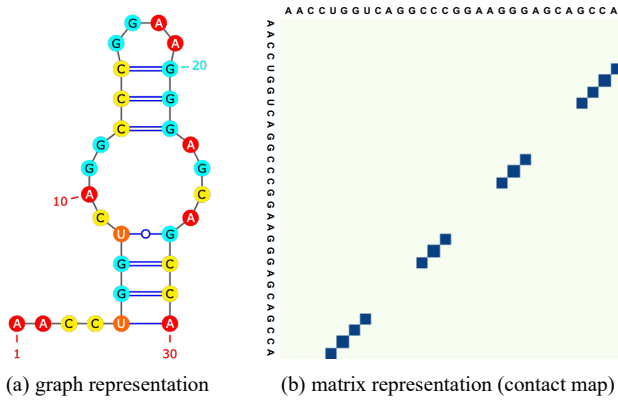


Figure 1. The graph and matrix representation of an RNA secondary structure example.

Computational RNA secondary structure prediction methods have been favoured for their high efficiency in recent years (Jorns et al., 2007). Currently, mainstream methods can be broadly classified into two categories (Rivas, 2013; Fu et al., 2022; Singh et al., 2019): (i) comparative sequence analysis and (ii) single sequence folding algorithm. Comparative sequence analysis determines the secondary structure conserved among homologous sequences but the limited known RNA families hinder its development (Knudsen & Hein, 1999; 2003; Hofacker et al., 2002; Gutell et al., 2002; Griffiths-Jones et al., 2003; Gardner et al., 2009; Nawrocki et al., 2015). Researchers thus resort to single RNA sequence folding algorithms that do not need multiple sequence alignment information. A classical category of computational RNA folding algorithms is to use dynamic programming (DP) that assumes the secondary structure is a result of energy minimization (Bellaousov et al., 2013; Nicholas & Zuker, 2008; Lorenz et al., 2011; Zuker, 2003; Mathews & Turner, 2006; Do et al., 2006). However, energy-based approaches usually require the base pairs have a nested structure while ignoring some valid yet biologically essential structures such as pseudoknots, i.e., non-nested base pairs (Chen et al., 2019; Seetin & Mathews, 2012; Xu & Chen, 2015), as shown in Fig. 2. Since predicting secondary structures with pseudoknots under the energy minimization framework has shown to be hard and NP-complete (Wang & Tian, 2011; Fu et al., 2022), deep

<sup>\*</sup>Equal contribution <sup>1</sup>Zhejiang University <sup>2</sup>AI Research and Innovation Lab, Westlake University. Correspondence to: Stan Z. Li <Stan.ZQ.Li@westlake.edu.cn>, Cheng Tan <tancheng@westlake.edu.cn>.

learning techniques are introduced as an alternative.

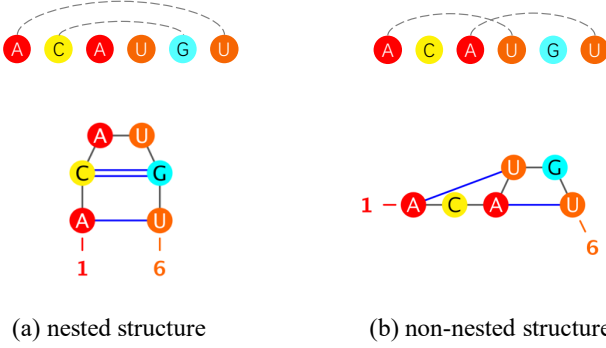


Figure 2. Examples of nested and non-nested secondary structures.

Attempts to overcome the limitations of energy-based methods have motivated deep learning methods that predict RNA secondary structures in the absence of DP. SPOT-RNA (Singh et al., 2019) is a seminal work that ensembles ResNet (He et al., 2016) and LSTM (Hochreiter & Schmidhuber, 1997) and applies transfer learning to identify molecular recognition features. SPOT-RNA does not constrain the output space into valid RNA secondary structures, which degrades its generalization ability on new datasets (Jung et al.). E2Efold (Chen et al., 2019) employs an unrolled algorithm for constrained programming that post-processes the network output to satisfy the constraints. E2Efold introduces a convex relaxation to make the constrained optimization tractable, leading to possible structural constraint violations and poor generalization ability (Sato et al., 2021; Fu et al., 2022). Developing an appropriate post-processing step that forces the output to be valid become an important issue.

Apart from the post-processing step, state-of-the-art approaches require hand-crafted features and introduce the pre-processing step for such features, which is inefficient and needs expert knowledge. CDPfold (Zhang et al., 2019) develops a matrix representation based on sequence pairing that reflects the implicit matching between bases. UFold (Fu et al., 2022) follows the exact post-process mechanism as E2Efold and uses hand-crafted features from CDPfold with U-Net (Ronneberger et al., 2015) model architecture to improve the performance.

Though promising, current deep learning methods (Tan et al., 2021; 2022d; c; e; a; b; Gao et al., 2022f; 2021; 2022a; d; c; e; b; Cao et al., 2022; Liu et al., 2022; Hu et al., 2022; Xia et al., 2022) on RNA secondary structure prediction have been distressed by: (1) the post-processing step that is complicated and poor in generalization and (2) the pre-processing step that requires expensive complexity and expert knowledge. In this paper, we present RFold, a simple yet effective RNA secondary structure prediction method in an end-to-end manner. Specifically, we introduce a novel *Row-Col Softmax* that performs row-wise and col-wise Softmax functions for

symmetrized metrics to replace the complicated constrained optimization-based post-processing step. Owing to the differentiable property of the Row-Col Softmax, we can apply a corresponding *Row-Col Argmax* function to get accurate and valid final outputs. Besides, we adopt attention maps as informative representations to automatically learn the pairwise interactions of the nucleotide bases instead of using hand-crafted features as the pre-processing step.

We conduct extensive experiments to compare RFold with state-of-the-art methods on several benchmark datasets and show the superior performance of our proposed method. Moreover, RFold has faster inference efficiency than those methods due to its simplicity.

## 2. Related work

### 2.1. Comparative Sequence Analysis

Comparative sequence analysis determines base pairs conserved among homologous sequences (Singh et al., 2019; Gardner & Giegerich, 2004). RNAalifold (Hofacker et al., 2002) implements an extension of the Zuker-Stiegler algorithm for computing a consensus structure from RNA alignments. Pfold (Knudsen & Hein, 2003; 1999) employs a stochastic context-free grammar to produce a prior probability distribution of RNA structures. ILM (Ruan et al., 2004) combines thermodynamic and mutual information content scores for predicting complicated structures. Sankoff (Hofacker et al., 2004) merges the sequence alignment and maximal-pairing folding methods (Nussinov et al., 1978). Dynalign (Mathews & Turner, 2002) and Carnac (Touzet & Perriquet, 2004; Perriquet et al., 2003) are the subsequent variants of Sankoff algorithms. Foldalign (Gorodkin et al., 1997; 2001) is a mixture of local alignment and maximum number of base-pairs algorithm. RNA forester (Hochsmann et al., 2003) introduces a tree alignment model for global and local alignments. However, the number of known RNA families in Rfam (Griffiths-Jones et al., 2003; Gardner et al., 2009; Nawrocki et al., 2015) is limited, which impedes the development of comparative methods.

### 2.2. Energy-based Folding Algorithms

When the secondary structure contains only nested base pairing, energy minimization through dynamic programming can efficiently make the prediction. Vienna RNAfold (Lorenz et al., 2011), Mfold (Zuker, 2003), RNAsstructure (Mathews & Turner, 2006) and CONTRAfold (Do et al., 2006) are the early works belonging to this category. Faster implementations that speed up the dynamic programming are then proposed, e.g., Vienna RNAlignfold (Bernhart et al., 2006), LocalFold (Lange et al., 2012), and LinearFold (Huang et al., 2019). However, these methods cannot well solve the secondary structure prediction with pseudo-

knots because predicting the lowest free energy structures with pseudoknots are NP-complete (Lyngsø & Pedersen, 2000), making it difficult to improve the performance.

### 2.3. Learning-based Folding Algorithms

SPOT-RNA (Singh et al., 2019) is a seminal work that employs deep learning for RNA secondary structure prediction. SPOT-RNA2 (Singh et al., 2021) improves its predecessor by using evolution-derived sequence profiles and mutational coupling. Inspired by Raptor-X (Wang et al., 2017) and SPOT-Contact (Hanson et al., 2018), SPOT-RNA uses ResNet and bidirectional LSTM with a sigmoid function to output the secondary structures. MXfold (Akiyama et al., 2018) is also an early work that combines support vector machines and thermodynamic models. CDPfold (Zhang et al., 2019), DMFold (Wang et al., 2019), and MXFold2 (Sato et al., 2021) integrate deep learning techniques with energy-based methods. E2Efold (Chen et al., 2019) takes a remarkable step in constraining the output to be valid by learning unrolled algorithms. However, its relaxation for making the optimization tractable may violate the structural constraints. UFold (Fu et al., 2022) further recognizes secondary structure prediction problem as image segmentation and introduces U-Net model architecture to solve it. In this work, our proposed RFold introduces a novel Row-Col Softmax activation function for optimizing the output, which can guarantee it to be valid.

### 2.4. Sequence-to-map Transformations

In RNA secondary structure prediction, a one-dimensional sequence is given to predict its corresponding two-dimensional secondary structure, represented by a contact map. This process inevitably involves a sequence-to-map transformation. SPOT-RNA (Singh et al., 2019) and E2Efold (Chen et al., 2019) apply an outer concatenation that directly concatenates the pair-wise sequence embeddings for the sequence-to-map transformation. Such straightforward embeddings may be less informative. CDPfold (Zhang et al., 2019) develops hand-crafted feature maps that contain the pairing probability between input base pairs calculated by specific rules. UFold (Fu et al., 2022) further designs feature maps to denote the occurrences of one of the sixteen possible base pairs between the nucleotides. In this work, our RFold adopts the attention map of sequence embeddings to automatically generate informative feature maps from given sequences.

## 3. Preliminaries and Backgrounds

### 3.1. Preliminaries

The primary structure of RNA is the ordered linear sequence of bases, typically notated as a string of letters. Formally,

an RNA sequence can be represented as  $\mathbf{X} = (x_1, \dots, x_L)$ , where  $x_i \in \{A, U, C, G\}$  denotes one of four bases, i.e., *Adenine* (A), *Uracil* (U), *Cytosine* (C), and *Guanine* (G). The secondary structure of RNA is a contact map represented by a matrix  $\mathbf{M} \in \{0, 1\}^{L \times L}$ , where  $M_{ij} = 1$  if the  $i$ -th and  $j$ -th bases are paired. In the RNA secondary structure prediction problem, we aim to obtain a model with learnable parameters  $\Theta$  that learns a mapping  $\mathcal{F}_\Theta : \mathbf{X} \mapsto \mathbf{M}$  by exploring the interactions between bases. Here, we decompose the mapping  $\mathcal{F}_\Theta$  into two sub-mappings as:

$$\mathcal{F}_\Theta := \mathcal{H}_{\theta_h} \circ \mathcal{G}_{\theta_g}, \quad (1)$$

where  $\mathcal{H}_{\theta_h} : \mathbf{X} \mapsto \mathbf{H}$ ,  $\mathcal{G}_{\theta_g} : \mathbf{H} \mapsto \mathbf{M}$  are mappings parameterized by  $\theta_h$  and  $\theta_g$ , respectively.  $\mathbf{H} \in \mathbb{R}^{L \times L}$  can be regarded as the unconstrained output of neural networks.

### 3.2. Backgrounds

It is worth noting that there are hard constraints on the formation of RNA secondary structure, i.e., certain kinds of pairing are not available (Steeg, 1993). These constraints (Chen et al., 2019) can be formally described as:

- (a) Only three types of nucleotide combinations can form base pairs. Given the available nucleotide combinations  $\mathcal{B} := \{AU, UA\} \cup \{GC, CG\} \cup \{GU, UG\}$ ,  $\forall i, j$ , if the base pair  $x_i x_j \notin \mathcal{B}$ , then  $M_{ij} = 0$ .
- (b) No sharp loops within three bases. For arbitrary adjacent bases, there is no pairing between them, i.e.,  $\forall |i - j| \leq 3, M_{ij} = 0$ .
- (c) There is a single pair for each base at most, i.e.,  $\forall i, \sum_{j=1}^L M_{ij} \leq 1$ .

The available space of valid secondary structures are all *symmetric* matrices  $\mathbf{M} \in \{0, 1\}^{L \times L}$  that satisfy the above three constraints. The first two constraints can be satisfied by a simple way. We define a constraint matrix  $\bar{\mathbf{M}}$  as  $\bar{M}_{ij} := 1$  if  $x_i x_j \in \mathcal{B}$  and  $|i - j| \geq 4$ , and  $\bar{M}_{ij} := 0$  otherwise. By element-wise multiplication of the network output and the constraint matrix  $\bar{\mathbf{M}}$ , invalid pairs are masked.

*The critical issue of obtaining a valid RNA secondary structure is processing the network output to be a symmetric binary matrix that only a single "1" is allowed to exist in each row and each column.* There are different strategies for dealing with this issue.

**SPOT-RNA** is a typical kind of method that impose the minor constraint. Given the original output of neural networks  $\mathbf{H}$ , it directly applies the Sigmoid function, assigning 1 and 0 to values that greater than and less than 0.5, respectively. Formally, this process can be represented as:

$$\mathcal{G}(\mathbf{H}) = \mathbb{1}_{[\text{Sigmoid}(\mathbf{H}) > s]} \odot \mathbf{H}. \quad (2)$$

where  $s$  is an offset term that is set as 0.5 here. None of the constraints mentioned above are explicitly imposed, and no extra parameters  $\theta_g$  are in need.

**E2Efold** formulates the problem with constrained optimization and introduces an intermediate variable  $\hat{\mathbf{A}} \in \mathbb{R}^{L \times L}$ . It aims to maximize the predefined score function:

$$\mathcal{S}(\mathbf{H}, \hat{\mathbf{A}}) = \max_{\hat{\mathbf{A}} \in \mathbb{R}^{L \times L}} \frac{1}{2} \left\langle \mathbf{H} - s, \mathcal{T}(\hat{\mathbf{A}}) \right\rangle - \rho \|\hat{\mathbf{A}}\|_1, \quad (3)$$

where  $\mathcal{T}(\hat{\mathbf{A}}) = \frac{1}{2}(\hat{\mathbf{A}} \odot \hat{\mathbf{A}} + (\hat{\mathbf{A}} \odot \hat{\mathbf{A}})^T) \odot \bar{\mathbf{M}}$  ensures the output is a symmetric matrix that satisfies the constraints (a-b),  $s$  is an offset term that is set as  $\log(9.0)$  here,  $\langle \cdot, \cdot \rangle$  denotes matrix inner product, and  $\rho \|\hat{\mathbf{A}}\|_1$  is a  $\ell_1$  penalty term to make the matrix to be sparse.

The constraint (c) is imposed by requiring Eq. 3 to satisfy  $\mathcal{T}(\hat{\mathbf{A}}) \mathbf{1} \leq \mathbf{1}$ . Thus, Eq. 3 is rewritten as:

$$\begin{aligned} \mathcal{S}(\mathbf{H}, \hat{\mathbf{A}}) = \min_{\lambda \geq 0} \max_{\hat{\mathbf{A}} \in \mathbb{R}^{L \times L}} & \frac{1}{2} \left\langle \mathbf{H} - s, \mathcal{T}(\hat{\mathbf{A}}) \right\rangle - \rho \|\hat{\mathbf{A}}\|_1 \\ & - \left\langle \lambda, \text{ReLU}(\mathcal{T}(\hat{\mathbf{A}}) \mathbf{1} - \mathbf{1}) \right\rangle, \end{aligned} \quad (4)$$

where  $\lambda \in \mathbb{R}_+^L$  is a Lagrange multiplier.

Formally, this process can be represented as:

$$\mathcal{G}_{\theta_g}(\mathbf{H}) = \mathcal{T}(\arg \min_{\hat{\mathbf{A}} \in \mathbb{R}^{L \times L}} \mathcal{S}(\mathbf{H}, \hat{\mathbf{A}})) \quad (5)$$

Though three constraints are explicitly imposed in E2Efold, this method requires iterative steps to approximate the valid solutions and cannot guarantee that the results are entirely valid. Moreover, it needs a set of parameters  $\theta_g$  in this processing, making tuning the model complex.

## 4. RFold

### 4.1. Row-Col Softmax

To obtain valid structures that satisfy the three constraints in a simple yet effective manner, we propose a Row-Col Softmax activation function. *The motivation for this comes from the fact that if each base has at most one pair, then the value "1" should be the maximum value on its row and column.* In other words, we aim to obtain a processed matrix  $\mathcal{G}(\mathbf{H})$  where, if there is a pairing between the base  $i$  and base  $j$ , its corresponding value  $\mathcal{G}(\mathbf{H})_{ij}$  should be the maximum value of its row and column.

We first construct a symmetric matrix  $\hat{\mathbf{H}} \in \mathbb{R}^{L \times L}$  based on the network output:

$$\hat{\mathbf{H}} = \mathbf{H} \odot \mathbf{H}^T. \quad (6)$$

Then, row-wise Softmax and column-wise Softmax on the

symmetric matrix  $\hat{\mathbf{H}}$  are performed separately:

$$\begin{aligned} \text{Row-Softmax}(\hat{\mathbf{H}}_{ij}) &= \frac{\exp(\hat{\mathbf{H}}_{ij})}{\sum_{k=1}^L \exp(\hat{\mathbf{H}}_{ik})}, \\ \text{Col-Softmax}(\hat{\mathbf{H}}_{ij}) &= \frac{\exp(\hat{\mathbf{H}}_{ij})}{\sum_{k=1}^L \exp(\hat{\mathbf{H}}_{kj})}. \end{aligned} \quad (7)$$

The Row-Col Softmax activation function is defined as the average of the row-wise Softmax and column-wise Softmax:

$$\begin{aligned} \text{Row-Col-Softmax}(\hat{\mathbf{H}}_{ij}) &= \frac{1}{2}(\text{Row-Softmax}(\hat{\mathbf{H}}_{ij}) + \text{Col-Softmax}(\hat{\mathbf{H}}_{ij})), \end{aligned} \quad (8)$$

**Theorem 1.** Given a symmetric matrix  $\hat{\mathbf{H}} \in \mathbb{R}^{L \times L}$ , the matrix Row-Col-Softmax( $\hat{\mathbf{H}}$ ) is also a symmetric matrix.

*Proof:* See Appendix B.1.

As shown in Fig. 3, taking a random symmetric  $6 \times 6$  matrix as an example, we show the output matrices of Row-Softmax, Col-Softmax, and Row-Col-Softmax functions, respectively. It can be seen that the output matrix of Row-Col-Softmax is still a symmetric matrix. Leveraging the differentiable property of Row-Col-Softmax, the model can be easily optimized.

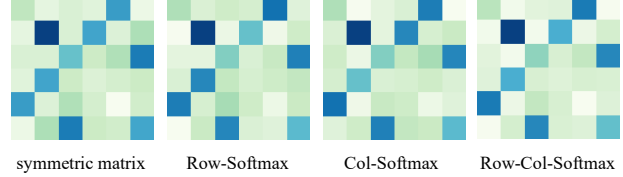


Figure 3. The visualization of the Row-Col-Softmax function. Note that here we do not take constraints (a-b) into consideration for convenience.

In the training phase, we apply the differentiable Row-Col Softmax activation function at the end of the model:

$$\mathcal{G}(\mathbf{H}) = \text{Row-Col-Softmax}(\mathbf{H} \odot \mathbf{H}^T) \odot \bar{\mathbf{M}} \quad (9)$$

The loss function is the mean square error (MSE) between  $\mathcal{G}(\mathbf{H})$  and  $\mathbf{M}$ :

$$\mathcal{L}(\mathcal{G}(\mathbf{H}), \mathbf{M}) = \frac{1}{L^2} \|\mathcal{G}(\mathbf{H}) - \mathbf{M}\|^2. \quad (10)$$

### 4.2. Row-Col Argmax

In the evaluation phase, we introduce a Row-Col Argmax function analogy to the Row-Col Softmax function:

$$\begin{aligned} \text{Row-Col-Argmax}(\hat{\mathbf{H}}) &= \text{Row-Argmax}(\hat{\mathbf{H}}) \odot \text{Col-Argmax}(\hat{\mathbf{H}}), \end{aligned} \quad (11)$$

where Row-Argmax and Col-Argmax are row-wise and column-wise Argmax functions that defined as:

$$\text{Row-Argmax}(\widehat{\mathbf{H}}_{ij}) = \begin{cases} 1, & \text{if } \max\{\widehat{\mathbf{H}}_{ik}\}_{k=1}^L = \widehat{\mathbf{H}}_{ij}, \\ 0, & \text{otherwise.} \end{cases}$$

$$\text{Col-Argmax}(\widehat{\mathbf{H}}_{ij}) = \begin{cases} 1, & \text{if } \max\{\widehat{\mathbf{H}}_{kj}\}_{k=1}^L = \widehat{\mathbf{H}}_{ij}, \\ 0, & \text{otherwise.} \end{cases}$$
(12)

**Theorem 2.** Given a symmetric matrix  $\widehat{\mathbf{H}} \in \mathbb{R}^{L \times L}$ , the matrix  $\text{Row-Col-Argmax}(\widehat{\mathbf{H}})$  is also a symmetric matrix.

*Proof:* See Appendix B.2.

As shown in Fig. 4, taking a random symmetric  $6 \times 6$  matrix as an example, we show the output matrices of Row-Argmax, Col-Argmax, and Row-Col-Argmax functions, respectively. The Row-Col Argmax select the value that has the maximum value on both its row and column while keeping the output matrix symmetric.

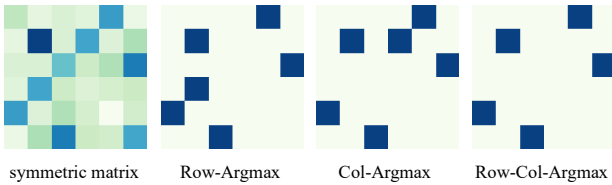


Figure 4. The visualization of the Row-Col-Argmax function. Note that here we do not take constraints (a-b) into consideration for convenience.

From Theorem 2, we can observe that  $\text{Row-Col-Argmax}(\widehat{\mathbf{H}})$  is a symmetric matrix that satisfies the constraint (c). By multiplying this matrix with the constrain matrix  $\bar{\mathbf{M}}$ , the constraints (a) and (b) can also be satisfied. Thus, the output at the evaluation phase is:

$$\mathcal{G}(\mathbf{H}) = \text{Row-Col-Argmax}(\mathbf{H} \odot \mathbf{H}^T) \odot \bar{\mathbf{M}}. \quad (13)$$

### 4.3. Seq2map Attention

To simplify the pre-processing step that constructs hand-crafted pair-wise features based on RNA sequences, we propose a Seq2map attention module that is able to automatically produce informative representations. As shown in Fig. 5, given a sequence in one-hot form  $\mathbf{X} \in \mathbb{R}^{L \times 4}$ , we first obtain the sum of the token embedding and positional embedding as the input of the Seq2map attention. We denote the input as  $\mathbf{Z} \in \mathbb{R}^{L \times D}$  for convenience, where  $D$  is the hidden layer size of the token and positional embeddings.

Motivated by the recent progress in attention mechanisms (Vaswani et al., 2017; Dauphin et al., 2017; Kitaev et al., 2019; Choromanski et al., 2020; Katharopoulos et al., 2020; Qin et al., 2021; Hua et al., 2022; Wu et al., 2022; Li

et al., 2022), we aim to develop a highly effective sequence-to-map transformation based on pair-wise attention. We obtain the query  $\mathbf{Q} \in \mathbb{R}^{L \times D}$  and key  $\mathbf{K} \in \mathbb{R}^{L \times D}$  by applying per-dim scalars and offsets to  $\mathbf{Z}$ :

$$\mathbf{Q} = \gamma_Q \mathbf{Z} + \beta_Q, \quad (14)$$

$$\mathbf{K} = \gamma_K \mathbf{Z} + \beta_K,$$

where  $\gamma_Q, \gamma_K, \beta_Q, \beta_K \in \mathbb{R}^{1 \times D}$  are learnable parameters.

Then, the pair-wise attention map is obtained by:

$$\bar{\mathbf{Z}} = \text{ReLU}^2(\mathbf{Q}\mathbf{K}^T/L), \quad (15)$$

where  $\text{ReLU}^2$  is an activation function that can be recognized as a simplified Softmax function in vanilla Transformers (So et al., 2021). The output of Seq2map is the gated representation of  $\bar{\mathbf{Z}}$ , which has been proven effective in many cases (Dauphin et al., 2017; Shazeer, 2020; Narang et al., 2021):

$$\hat{\mathbf{Z}} = \bar{\mathbf{Z}} \odot \sigma(\bar{\mathbf{Z}}), \quad (16)$$

where  $\sigma(\cdot)$  is the Sigmoid function that performs as a gate.

Analogous to (Fu et al., 2022), we identify the problem of predicting  $\mathbf{H} \in \mathbb{R}^{L \times L}$  from the given sequence attention map  $\hat{\mathbf{Z}} \in \mathbb{R}^{L \times L}$  as an image-to-image segmentation problem and apply the U-Net model architecture to extract pair-wise information, as shown in Fig. 5.

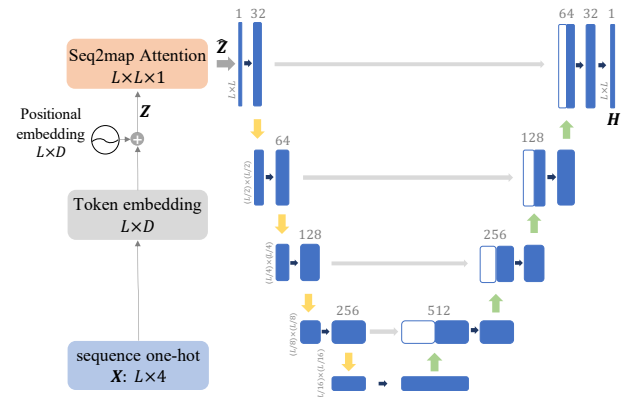


Figure 5. The overview model architecture of RFold.

## 5. Experiments

We conduct experiments to compare our proposed RFold with state-of-the-art and commonly used methods in the field of RNA secondary structure prediction. Multiple experimental settings are taken into account, including standard RNA secondary structure prediction, generalization evaluation, large-scale benchmark evaluation, and inference time comparison. Ablation studies are also presented.

**Datasets** We use three benchmark datasets: (i) RNAsralign (Tan et al., 2017), one of the most comprehensive collections of RNA structures, is composed of 37,149 structures from 8 RNA types; (ii) ArchiveII (Sloma & Mathews, 2016), a widely used benchmark dataset in classical RNA folding methods, containing 3,975 RNA structures from 10 RNA types; (iii) bpRNA (Singh et al., 2019), is a large scale benchmark dataset, containing 102,318 structures from 2,588 RNA types.

**Baselines** We compare our proposed RFold with baslines including: energy-based folding methods such as Mfold (Zuker, 2003), RNAssoft (Andronescu et al., 2003), RNAfold (Lorenz et al., 2011), RNAstructure (Mathews & Turner, 2006), CONTRAfold (Do et al., 2006), Contextfold (Zakov et al., 2011), and LinearFold (Huang et al., 2019); learning-based folding methods such as SPOT-RNA (Singh et al., 2019), CDPfold (Zhang et al., 2019), Externafold (Wayment-Steele et al., 2021), E2Efold (Chen et al., 2019), MXfold2 (Sato et al., 2021), and UFold (Fu et al., 2022).

**Metrics** We evaluate the performance by precision, recall, and F1 score, which are defined as:

$$\text{Precision} = \frac{\text{TP}}{\text{TP} + \text{FP}}, \text{Recall} = \frac{\text{TP}}{\text{TP} + \text{FN}}, \quad (17)$$

$$\text{F1} = 2 \frac{\text{Precision} \cdot \text{Recall}}{\text{Precision} + \text{Recall}},$$

where TP, FP, and FN denote true positive, false positive and false negative, respectively.

**Implementation details** Following (Fu et al., 2022), we train the model for 100 epochs with the Adam optimizer. The learning rate is set as 0.001, and the batch size is 1 for sequences with different lengths.

### 5.1. Standard RNA Secondary Structure Prediction

Following (Chen et al., 2019), we split the original RNAsralign dataset into training, validation, and testing sets by stratified sampling to ensure every set has all RNA types. We train the model on the training set of RNAsralign and evaluate the performance on its testing set by using the best model learned from its validation set for fair comparisons across various methods.

We report the experimental results in Table 1. It can be seen that energy-based methods can achieve relatively weak F1 scores ranging from 0.420 (Mfold) to 0.633 (CONTRAfold).

Learning-based folding algorithms like E2Efold and UFold can significantly improve performance by large margins, while our proposed RFold obtain even better performance among all the three metrics. Moreover, RFold obtains

Table 1. Results on RNAsralign test set. Results in bold and underlined are the top-1 and top-2 performances, respectively.

Method	Precision	Recall	F1
Mfold	0.450	0.398	0.420
RNAfold	0.516	0.568	0.540
RNAstructure	0.537	0.568	0.550
CONTRAfold	0.608	0.663	0.633
LinearFold	0.620	0.606	0.609
CDPfold	0.633	0.597	0.614
E2Efold	0.866	0.788	0.821
UFold	<u>0.905</u>	<u>0.927</u>	<u>0.915</u>
RFold	<b>0.981</b>	<b>0.973</b>	<b>0.977</b>

about 8% higher precision than the state-of-the-art method UFold. This phenomenon suggests that our proposed row-col Argmax function is strict to satisfy all the hard constraints for predicting valid structures.

### 5.2. Generalization Evaluation

To verify the generalization ability of our proposed RFold, we directly evaluate the performance on another benchmark dataset ArchiveII using the pre-trained model on the RNAsralign training dataset. Following (Chen et al., 2019), we exclude RNA sequences in ArchiveII that have overlapping RNA types with the RNAsralign dataset for a fair comparison. The results are reported in Table 2.

It can be seen that traditional methods achieve F1 scores in the range of 0.545 to 0.842. A recent learning-based method, MXfold2, obtains the F1 score of 0.768, which is even lower than some energy-based methods. Another state-of-the-art learning-based method improves the performance to the F1 score of 0.905. RFold further improves the F1 score to 0.921, even higher than UFold. It is worth noting that RFold has a relatively lower result in the recall metric and a significantly higher result in the precision metric. The reason for this phenomenon may be the strict constraints of RFold. While none of the current learning-based methods can satisfy all the constraints we introduced in Sec. 3.2, the predictions of RFold are guaranteed to be valid. Thus, RFold may cover fewer pair-wise interactions, leading to a lower recall metric. However, the highest F1 score still suggests the great generalization ability of RFold.

### 5.3. Large-scale Benchmark Evaluation

The large-scale benchmark dataset bpRNA has a fixed training set (TR0), evaluation set (VL0), and testing set (TS0). Following (Singh et al., 2019; Sato et al., 2021; Fu et al., 2022), we train the model in bpRNA-TR0 and evaluate the performance on bpRNA-TS0 by using the best model learned from bpRNA-VL0. Due to the originally reported

Table 2. Results on ArchiveII dataset. Results in bold and underlined are the top-1 and top-2 performances, respectively.

Method	Precision	Recall	F1
Mfold	0.668	0.590	0.621
CDPfold	0.557	0.535	0.545
RNAfold	0.663	0.613	0.631
RNAstructure	0.664	0.606	0.628
CONTRAFold	0.696	0.651	0.665
LinearFold	0.724	0.605	0.647
RNAsoft	0.665	0.594	0.622
Eternafold	0.667	0.622	0.636
E2Efold	0.734	0.660	0.686
SPOT-RNA	0.743	0.726	0.711
MXfold2	0.788	0.760	0.768
Contextfold	0.873	0.821	0.842
UFold	<u>0.887</u>	<b>0.928</b>	<u>0.905</u>
RFold	<b>0.938</b>	<u>0.910</u>	<b>0.921</b>

results of UFold being obtained by involving more training data, we reproduce its results by training the UFold model with the only pure bpRNA-TR0 dataset. We summarize the evaluation results in Table 3.

It can be seen that RFold significantly improves the previous state-of-the-art method SPOT-RNA by 4.0% in the F1 score. The precision metric is consistently better than baseline models, which benefits the F1 score. The strict constraints still limit the recall metric. In general, with the highest F1 score among these baseline models, RFold can be a valuable method for further development of the RNA secondary structure prediction field.

Table 3. Results on bpRNA-TS0 set. Results in bold and underlined are the top-1 and top-2 performances, respectively.

Method	Precision	Recall	F1
E2Efold	0.140	0.129	0.130
RNAstructure	0.494	0.622	0.533
RNAsoft	0.497	0.626	0.535
RNAfold	0.494	0.631	0.536
Mfold	0.501	0.627	0.538
Contextfold	0.529	0.607	0.546
LinearFold	0.561	0.581	0.550
MXfold2	0.519	0.646	0.558
Externafold	0.516	<u>0.666</u>	0.563
CONTRAFold	0.528	0.655	0.567
SPOT-RNA	<u>0.594</u>	<b>0.693</b>	<u>0.619</u>
UFold	0.521	0.588	0.553
RFold	<b>0.692</b>	0.635	<b>0.644</b>

Following (Fu et al., 2022), we conduct an experiment on long-rage interactions. The bpRNA-TS0 dataset contains more versatile RNA sequences of different lengths and var-

ious types, which can be a reliable evaluation. Given a sequence of length  $L$ , the long-range base pairing is defined as the the paired and unpaired bases with intervals longer than  $L/2$ . The precision, recall, and F1 scores are calculated under such an experimental setting. As shown in Table 4, RFold performs unexpectedly well on these long-range base pairing predictions. We can also find that UFold performs better in long-range cases than the complete cases. The possible reason may comes from the U-Net model architecture that learn multi-scale features. RFold significantly improves UFold in all the metrics by large margins, demonstrating its strong predictive ability.

Table 4. Results on long-range bpRNA-TS0 set. Results in bold and underlined are the top-1 and top-2 performances, respectively.

Method	Precision	Recall	F1
Mfold	0.315	0.450	0.356
RNAfold	0.304	0.448	0.350
RNAstructure	0.299	0.428	0.339
CONTRAFold	0.306	0.439	0.349
LinearFold	0.281	0.355	0.305
RNAsoft	0.310	0.448	0.353
Externafold	0.308	0.458	0.355
SPOT-RNA	0.361	0.492	0.403
MXfold2	0.318	0.450	0.360
Contextfold	0.332	0.432	0.363
UFold	<u>0.543</u>	<u>0.631</u>	<u>0.584</u>
RFold	<b>0.803</b>	<b>0.765</b>	<b>0.701</b>

#### 5.4. Inference Time Comparison

We compare the running time of different RNA secondary structure prediction methods for predicting on the testing set of RNASTralign. We report the average inference time per sequence in Table 5.

It can be seen that our proposed RFold obtains superior performance in time complexity. The fastest energy-based method is LinearFold, which needs an average of about 0.43s for each sequence. Moreover, the previous learning-based baseline method, UFold, needs an average of about 0.16s for each sequence. RFold has the highest inference speed, costing only about 0.02s per sequence. In particular, the inference speed is about eight times faster than UFold and sixteen times faster than MXfold2. The fast inference time of RFold benefits from its simplified sequence-to-map transformation in the pre-processing step.

#### 5.5. Ablation Study

**Rol-Col Softmax/Argmax** To validate the effectiveness of our proposed Rol-Col Softmax/Argmax functions, we conduct an experiment that replaces them with other post-

Table 5. Inference time on the RNAsRalign test set. Results in bold and underlined are the top-1 and top-2 performances, respectively.

Method	Time
CDPfold (Tensorflow)	300.11 s
RNAstructure (C)	142.02 s
CONTRAfold (C++)	30.58 s
Mfold (C)	7.65 s
Eternafold (C++)	6.42 s
RNAsoft (C++)	4.58 s
RNAfold (C)	0.55 s
LinearFold (C++)	0.43 s
SPOT-RNA(Pytorch)	77.80 s (GPU)
E2Efold (Pytorch)	0.40 s (GPU)
MXfold2 (Pytorch)	0.31 s (GPU)
UFold (Pytorch)	0.16 s (GPU)
RFold (Pytorch)	<b>0.02 s (GPU)</b>

processing methods. The results are summarized in Table 6, where RFold-E and RFold-S denote our model with the post-processing strategies of E2Efold and SPOT-RNA, respectively. While precision, recall, and F1 score are evaluated at base-level, we report the validity that is a sample-level metric evaluating whether the predicted structure satisfies all the constraints. It can be seen that though RFold-E has comparable performance in the first three metrics with ours, many of its predicted structures are invalid. The post-processing strategy of SPOT-RNA has incorporated no constraint that results in its low validity. Moreover, its strategy seems to not fit our model well, which may be caused by the simplicity of our RFold model.

Table 6. Ablation study on different post-processing strategies (RNAsRalign testing set).

Method	Precision	Recall	F1	Validity
RFold	<b>0.981</b>	<b>0.973</b>	<b>0.977</b>	<b>100.00%</b>
RFold-E	0.888	0.906	0.896	50.31%
RFold-S	0.223	0.988	0.353	0.00%

**Seq2map Attention** We also conduct an experiment to evaluate the proposed Seq2map attention. We replace the Seq2map attention with the hand-crafted features from UFold and the outer concatenation from SPOT-RNA, which are denoted as RFold-U and RFold-SS, respectively. In addition to performance metrics, we also report the average inference time for each RNA sequence to evaluate the model complexity. We summarize the result in Table 7. It can be seen that RFold-U takes much more inference time than our RFold and RFold-SS due to the heavy computational cost when loading and learning from hand-crafted features. Moreover, it is surprising to find that RFold-SS has a little

better performance than RFold-U, with the least inference time for its simple outer concatenation operation. However, neither RFold-U nor RFold-SS can provide as informative representations like our proposed Seq2map attention. With comparable inference time with the simplest RFold-SS, our RFold outperforms baselines by large margins.

Table 7. Ablation study on different pre-processing strategies (RNAsRalign testing set).

Method	Precision	Recall	F1	Time
RFold	<b>0.981</b>	<b>0.973</b>	<b>0.977</b>	0.0167
RFold-U	0.875	0.941	0.906	0.0507
RFold-SS	0.886	0.945	0.913	<b>0.0158</b>

## 5.6. Visualization

We visualize two examples predicted by RFold and UFold in Fig. 6. The corresponding F1 scores are denoted at the bottom right of each plot. The first column of secondary structures is a simple example of a nested structure. It can be seen that UFold may fail in such a case. The second column of secondary structures is much more difficult that contains over 300 bases of the non-nested structure. While UFold fails in such a complex case, RFold can predict the structure accurately. Due to the limited space, we provide more visualization comparisons in Appendix C.

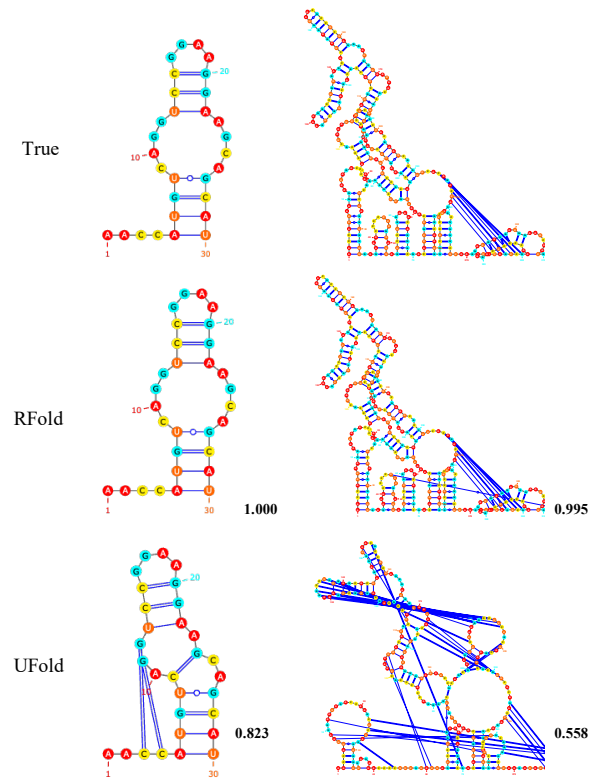


Figure 6. Visualization of the true and predicted structures.

## 6. Conclusion

In this study, we present RFold, a simple yet effective learning-based model for RNA secondary structure prediction. We propose Row-Col Softmax and Row-Col Argmax function to replace the complicated post-processing step while incorporating constraints for the output. Seq2map attention is proposed for sequence-to-map transformation, which can automatically learn informative representations from a single sequence without extensive pre-processing steps. Comprehensive experiments demonstrate that RFold achieves competitive performance with faster inference speed. We hope RFold can provide a new perspective for efficient RNA secondary structure prediction.

## Acknowledgements

Acknowledgement This work is supported by the Science and Technology Innovation 2030 - Major Project (No. 2021ZD0150100) and National Natural Science Foundation of China (No. U21A20427).

## References

- Akiyama, M., Sato, K., and Sakakibara, Y. A max-margin training of rna secondary structure prediction integrated with the thermodynamic model. *Journal of bioinformatics and computational biology*, 16(06):1840025, 2018.
- Andronescu, M., Aguirre-Hernandez, R., Condon, A., and Hoos, H. H. Rnasoft: a suite of rna secondary structure prediction and design software tools. *Nucleic acids research*, 31(13):3416–3422, 2003.
- Bellaousov, S., Reuter, J. S., Seetin, M. G., and Mathews, D. H. Rnastucture: web servers for rna secondary structure prediction and analysis. *Nucleic acids research*, 41(W1):W471–W474, 2013.
- Bernhart, S. H., Hofacker, I. L., and Stadler, P. F. Local rna base pairing probabilities in large sequences. *Bioinformatics*, 22(5):614–615, 2006.
- Cao, H., Tan, C., Gao, Z., Chen, G., Heng, P.-A., and Li, S. Z. A survey on generative diffusion model. *arXiv preprint arXiv:2209.02646*, 2022.
- Chen, X., Li, Y., Umarov, R., Gao, X., and Song, L. Rna secondary structure prediction by learning unrolled algorithms. In *International Conference on Learning Representations*, 2019.
- Cheong, H.-K., Hwang, E., Lee, C., Choi, B.-S., and Cheong, C. Rapid preparation of rna samples for nmr spectroscopy and x-ray crystallography. *Nucleic acids research*, 32(10):e84–e84, 2004.
- Choromanski, K. M., Likhosherstov, V., Dohan, D., Song, X., Gane, A., Sarlos, T., Hawkins, P., Davis, J. Q., Mo-hiuddin, A., Kaiser, L., et al. Rethinking attention with performers. In *International Conference on Learning Representations*, 2020.
- Crick, F. Central dogma of molecular biology. *Nature*, 227 (5258):561–563, 1970.
- Dauphin, Y. N., Fan, A., Auli, M., and Grangier, D. Language modeling with gated convolutional networks. In *International conference on machine learning*, pp. 933–941. PMLR, 2017.
- Do, C. B., Woods, D. A., and Batzoglou, S. Contrafold: Rna secondary structure prediction without physics-based models. *Bioinformatics*, 22(14):e90–e98, 2006.
- Fallmann, J., Will, S., Engelhardt, J., Grüning, B., Backofen, R., and Stadler, P. F. Recent advances in rna folding. *Journal of biotechnology*, 261:97–104, 2017.
- Fica, S. M. and Nagai, K. Cryo-electron microscopy snapshots of the spliceosome: structural insights into a dynamic ribonucleoprotein machine. *Nature structural & molecular biology*, 24(10):791–799, 2017.
- Fox, G. E. and Woese, C. R. 5s rna secondary structure. *Nature*, 256(5517):505–507, 1975.
- Fu, L., Cao, Y., Wu, J., Peng, Q., Nie, Q., and Xie, X. Ufold: fast and accurate rna secondary structure prediction with deep learning. *Nucleic acids research*, 50(3):e14–e14, 2022.
- Fürtig, B., Richter, C., Wöhner, J., and Schwalbe, H. Nmr spectroscopy of rna. *ChemBioChem*, 4(10):936–962, 2003.
- Gao, Z., Lin, H., Tan, C., Wu, L., Li, S., et al. Git: Clustering based on graph of intensity topology. *arXiv preprint arXiv:2110.01274*, 2021.
- Gao, Z., Tan, C., Li, S., et al. Alphadesign: A graph protein design method and benchmark on alphafolddb. *arXiv preprint arXiv:2202.01079*, 2022a.
- Gao, Z., Tan, C., and Li, S. Z. Pifold: Toward effective and efficient protein inverse folding. *arXiv preprint arXiv:2209.12643*, 2022b.
- Gao, Z., Tan, C., and Li, S. Z. Prodesign: Toward effective and efficient protein design. *arXiv e-prints*, pp. arXiv–2209, 2022c.
- Gao, Z., Tan, C., Wu, L., and Li, S. Z. Cosp: Co-supervised pretraining of pocket and ligand. *arXiv preprint arXiv:2206.12241*, 2022d.

- Gao, Z., Tan, C., Wu, L., and Li, S. Z. Semiretro: Semi-template framework boosts deep retrosynthesis prediction. *arXiv preprint arXiv:2202.08205*, 2022e.
- Gao, Z., Tan, C., Wu, L., and Li, S. Z. Simvp: Simpler yet better video prediction. In *Proceedings of the IEEE/CVF Conference on Computer Vision and Pattern Recognition*, pp. 3170–3180, 2022f.
- Gardner, P. P. and Giegerich, R. A comprehensive comparison of comparative rna structure prediction approaches. *BMC bioinformatics*, 5(1):1–18, 2004.
- Gardner, P. P., Daub, J., Tate, J. G., Nawrocki, E. P., Kolbe, D. L., Lindgreen, S., Wilkinson, A. C., Finn, R. D., Griffiths-Jones, S., Eddy, S. R., et al. Rfam: updates to the rna families database. *Nucleic acids research*, 37(suppl\_1):D136–D140, 2009.
- Geisler, S. and Coller, J. Rna in unexpected places: long non-coding rna functions in diverse cellular contexts. *Nature reviews Molecular cell biology*, 14(11):699–712, 2013.
- Gorodkin, J., Heyer, L. J., and Stormo, G. D. Finding the most significant common sequence and structure motifs in a set of rna sequences. *Nucleic acids research*, 25(18):3724–3732, 1997.
- Gorodkin, J., Stricklin, S. L., and Stormo, G. D. Discovering common stem-loop motifs in unaligned rna sequences. *Nucleic Acids Research*, 29(10):2135–2144, 2001.
- Griffiths-Jones, S., Bateman, A., Marshall, M., Khanna, A., and Eddy, S. R. Rfam: an rna family database. *Nucleic acids research*, 31(1):439–441, 2003.
- Gutell, R. R., Lee, J. C., and Cannone, J. J. The accuracy of ribosomal rna comparative structure models. *Current opinion in structural biology*, 12(3):301–310, 2002.
- Hanson, J., Paliwal, K., Litfin, T., Yang, Y., and Zhou, Y. Accurate prediction of protein contact maps by coupling residual two-dimensional bidirectional long short-term memory with convolutional neural networks. *Bioinformatics*, 34(23):4039–4045, 2018.
- He, K., Zhang, X., Ren, S., and Sun, J. Deep residual learning for image recognition. In *Proceedings of the IEEE conference on computer vision and pattern recognition*, pp. 770–778, 2016.
- Hochreiter, S. and Schmidhuber, J. Long short-term memory. *Neural computation*, 9(8):1735–1780, 1997.
- Hochsmann, M., Toller, T., Giegerich, R., and Kurtz, S. Local similarity in rna secondary structures. In *Computational Systems Bioinformatics. CSB2003. Proceedings of the 2003 IEEE Bioinformatics Conference. CSB2003*, pp. 159–168. IEEE, 2003.
- Hofacker, I. L., Fekete, M., and Stadler, P. F. Secondary structure prediction for aligned rna sequences. *Journal of molecular biology*, 319(5):1059–1066, 2002.
- Hofacker, I. L., Bernhart, S. H., and Stadler, P. F. Alignment of rna base pairing probability matrices. *Bioinformatics*, 20(14):2222–2227, 2004.
- Hu, B., Xia, J., Zheng, J., Tan, C., Huang, Y., Xu, Y., and Li, S. Z. Protein language models and structure prediction: Connection and progression, 2022.
- Hua, W., Dai, Z., Liu, H., and Le, Q. Transformer quality in linear time. In *International Conference on Machine Learning*, pp. 9099–9117. PMLR, 2022.
- Huang, L., Zhang, H., Deng, D., Zhao, K., Liu, K., Hendrix, D. A., and Mathews, D. H. Linearfold: linear-time approximate rna folding by 5'-to-3' dynamic programming and beam search. *Bioinformatics*, 35(14):i295–i304, 2019.
- Iorns, E., Lord, C. J., Turner, N., and Ashworth, A. Utilizing rna interference to enhance cancer drug discovery. *Nature reviews Drug discovery*, 6(7):556–568, 2007.
- Jung, A. J., Lee, L. J., Gao, A. J., and Frey, B. J. Rtfold: Rna secondary structure prediction using deep learning with domain inductive bias.
- Katharopoulos, A., Vyas, A., Pappas, N., and Fleuret, F. Transformers are rnns: Fast autoregressive transformers with linear attention. In *International Conference on Machine Learning*, pp. 5156–5165. PMLR, 2020.
- Kitaev, N., Kaiser, L., and Levskaya, A. Reformer: The efficient transformer. In *International Conference on Learning Representations*, 2019.
- Knudsen, B. and Hein, J. Rna secondary structure prediction using stochastic context-free grammars and evolutionary history. *Bioinformatics (Oxford, England)*, 15(6):446–454, 1999.
- Knudsen, B. and Hein, J. Pfold: Rna secondary structure prediction using stochastic context-free grammars. *Nucleic acids research*, 31(13):3423–3428, 2003.
- Lange, S. J., Maticzka, D., Möhl, M., Gagnon, J. N., Brown, C. M., and Backofen, R. Global or local? predicting secondary structure and accessibility in mrnas. *Nucleic acids research*, 40(12):5215–5226, 2012.
- Li, S., Wang, Z., Liu, Z., Tan, C., Lin, H., Wu, D., Chen, Z., Zheng, J., and Li, S. Z. Efficient multi-order gated aggregation network. *arXiv preprint arXiv:2211.03295*, 2022.

- Liu, Z., Li, S., Wang, G., Tan, C., Wu, L., and Li, S. Z. Decoupled mixup for data-efficient learning. *arXiv preprint arXiv:2203.10761*, 2022.
- Lorenz, R., Bernhart, S. H., Höner zu Siederdissen, C., Tafer, H., Flamm, C., Stadler, P. F., and Hofacker, I. L. Viennarna package 2.0. *Algorithms for molecular biology*, 6(1):1–14, 2011.
- Lyngsø, R. B. and Pedersen, C. N. Rna pseudoknot prediction in energy-based models. *Journal of computational biology*, 7(3-4):409–427, 2000.
- Mathews, D. H. and Turner, D. H. Dynalign: an algorithm for finding the secondary structure common to two rna sequences. *Journal of molecular biology*, 317(2):191–203, 2002.
- Mathews, D. H. and Turner, D. H. Prediction of rna secondary structure by free energy minimization. *Current opinion in structural biology*, 16(3):270–278, 2006.
- Narang, S., Chung, H. W., Tay, Y., Fedus, L., Févry, T., Matena, M., Malkan, K., Fiedel, N., Shazeer, N., Lan, Z., et al. Do transformer modifications transfer across implementations and applications? In *EMNLP*, 2021.
- Nawrocki, E. P., Burge, S. W., Bateman, A., Daub, J., Eberhardt, R. Y., Eddy, S. R., Floden, E. W., Gardner, P. P., Jones, T. A., Tate, J., et al. Rfam 12.0: updates to the rna families database. *Nucleic acids research*, 43(D1):D130–D137, 2015.
- Nicholas, R. and Zuker, M. Unafold: Software for nucleic acid folding and hybridization. *Bioinformatics*, 453:3–31, 2008.
- Noller, H. F. Structure of ribosomal rna. *Annual review of biochemistry*, 53(1):119–162, 1984.
- Nussinov, R., Pieczenik, G., Griggs, J. R., and Kleitman, D. J. Algorithms for loop matchings. *SIAM Journal on Applied mathematics*, 35(1):68–82, 1978.
- Perriquet, O., Touzet, H., and Dauchet, M. Finding the common structure shared by two homologous rnas. *Bioinformatics*, 19(1):108–116, 2003.
- Qin, Z., Sun, W., Deng, H., Li, D., Wei, Y., Lv, B., Yan, J., Kong, L., and Zhong, Y. cosformer: Rethinking softmax in attention. In *International Conference on Learning Representations*, 2021.
- Rich, A. and RajBhandary, U. Transfer rna: molecular structure, sequence, and properties. *Annual review of biochemistry*, 45(1):805–860, 1976.
- Rivas, E. The four ingredients of single-sequence rna secondary structure prediction. a unifying perspective. *RNA biology*, 10(7):1185–1196, 2013.
- Ronneberger, O., Fischer, P., and Brox, T. U-net: Convolutional networks for biomedical image segmentation. In *International Conference on Medical image computing and computer-assisted intervention*, pp. 234–241. Springer, 2015.
- Ruan, J., Stormo, G. D., and Zhang, W. An iterated loop matching approach to the prediction of rna secondary structures with pseudoknots. *Bioinformatics*, 20(1):58–66, 2004.
- Sato, K., Akiyama, M., and Sakakibara, Y. Rna secondary structure prediction using deep learning with thermodynamic integration. *Nature communications*, 12(1):1–9, 2021.
- Seetin, M. G. and Mathews, D. H. Rna structure prediction: an overview of methods. *Bacterial regulatory RNA*, pp. 99–122, 2012.
- Shazeer, N. Glu variants improve transformer. *arXiv preprint arXiv:2002.05202*, 2020.
- Singh, J., Hanson, J., Paliwal, K., and Zhou, Y. Rna secondary structure prediction using an ensemble of two-dimensional deep neural networks and transfer learning. *Nature communications*, 10(1):1–13, 2019.
- Singh, J., Paliwal, K., Zhang, T., Singh, J., Litfin, T., and Zhou, Y. Improved rna secondary structure and tertiary base-pairing prediction using evolutionary profile, mutational coupling and two-dimensional transfer learning. *Bioinformatics*, 37(17):2589–2600, 2021.
- Sloma, M. F. and Mathews, D. H. Exact calculation of loop formation probability identifies folding motifs in rna secondary structures. *RNA*, 22(12):1808–1818, 2016.
- So, D., Maíñe, W., Liu, H., Dai, Z., Shazeer, N., and Le, Q. V. Searching for efficient transformers for language modeling. *Advances in Neural Information Processing Systems*, 34:6010–6022, 2021.
- Steeg, E. W. Neural networks, adaptive optimization, and rna secondary structure prediction. *Artificial intelligence and molecular biology*, pp. 121–160, 1993.
- Tan, C., Xia, J., Wu, L., and Li, S. Z. Co-learning: Learning from noisy labels with self-supervision. In *Proceedings of the 29th ACM International Conference on Multimedia*, pp. 1405–1413, 2021.
- Tan, C., Gao, Z., Li, S., Xu, Y., and Li, S. Z. Temporal attention unit: Towards efficient spatiotemporal predictive learning. *arXiv preprint arXiv:2206.12126*, 2022a.

- Tan, C., Gao, Z., and Li, S. Z. Simvp: Towards simple yet powerful spatiotemporal predictive learning. *arXiv preprint arXiv:2211.12509*, 2022b.
- Tan, C., Gao, Z., and Li, S. Z. Target-aware molecular graph generation. *arXiv preprint arXiv:2202.04829*, 2022c.
- Tan, C., Gao, Z., Wu, L., Li, S., and Li, S. Z. Hyperspherical consistency regularization. In *Proceedings of the IEEE/CVF Conference on Computer Vision and Pattern Recognition*, pp. 7244–7255, 2022d.
- Tan, C., Gao, Z., Xia, J., and Li, S. Z. Generative de novo protein design with global context. *arXiv preprint arXiv:2204.10673*, 2022e.
- Tan, Z., Fu, Y., Sharma, G., and Mathews, D. H. Turbofold ii: Rna structural alignment and secondary structure prediction informed by multiple homologs. *Nucleic acids research*, 45(20):11570–11581, 2017.
- Touzet, H. and Perriquet, O. Carnac: folding families of related rnas. *Nucleic acids research*, 32(suppl\_2):W142–W145, 2004.
- Vaswani, A., Shazeer, N., Parmar, N., Uszkoreit, J., Jones, L., Gomez, A. N., Kaiser, Ł., and Polosukhin, I. Attention is all you need. *Advances in neural information processing systems*, 30, 2017.
- Wang, L., Liu, Y., Zhong, X., Liu, H., Lu, C., Li, C., and Zhang, H. Dmfold: A novel method to predict rna secondary structure with pseudoknots based on deep learning and improved base pair maximization principle. *Frontiers in genetics*, 10:143, 2019.
- Wang, S., Sun, S., Li, Z., Zhang, R., and Xu, J. Accurate de novo prediction of protein contact map by ultra-deep learning model. *PLoS computational biology*, 13(1): e1005324, 2017.
- Wang, X. and Tian, J. Dynamic programming for np-hard problems. *Procedia Engineering*, 15:3396–3400, 2011.
- Wayment-Steele, H. K., Kladwang, W., Strom, A. I., Lee, J., Treuille, A., Participants, E., and Das, R. Rna secondary structure packages evaluated and improved by high-throughput experiments. *BioRxiv*, pp. 2020–05, 2021.
- Westhof, E. and Fritsch, V. Rna folding: beyond watson–crick pairs. *Structure*, 8(3):R55–R65, 2000.
- Wu, H., Wu, J., Xu, J., Wang, J., and Long, M. Flowformer: Linearizing transformers with conservation flows. *arXiv preprint arXiv:2202.06258*, 2022.
- Xia, J., Zheng, J., Tan, C., Wang, G., and Li, S. Z. Towards effective and generalizable fine-tuning for pre-trained molecular graph models. *BioRxiv*, 2022.
- Xu, X. and Chen, S.-J. Physics-based rna structure prediction. *Biophysics reports*, 1(1):2–13, 2015.
- Zakov, S., Goldberg, Y., Elhadad, M., and Ziv-Ukelson, M. Rich parameterization improves rna structure prediction. *Journal of Computational Biology*, 18(11):1525–1542, 2011.
- Zhang, H., Zhang, C., Li, Z., Li, C., Wei, X., Zhang, B., and Liu, Y. A new method of rna secondary structure prediction based on convolutional neural network and dynamic programming. *Frontiers in genetics*, 10:467, 2019.
- Zuker, M. Mfold web server for nucleic acid folding and hybridization prediction. *Nucleic acids research*, 31(13): 3406–3415, 2003.

## A. Comparison of mainstream RNA secondary structure prediction methods

We compare RFold with other mainstream RNA secondary structure prediction methods and summarize the results in Table 8.

## B. Proofs of Theorems

### B.1. Proof of Theorem 1

**Theorem 1.** Given a symmetric matrix  $\widehat{\mathbf{H}} \in \mathbb{R}^{L \times L}$ , the matrix Row-Col-Softmax( $\widehat{\mathbf{H}}$ ) is also a symmetric matrix.

*Proof:*  $\forall i, j \in \{1, \dots, L\}$ ,

$$\begin{aligned}
 & \text{Row-Col-Softmax}(\widehat{\mathbf{H}}_{ji}) \\
 &= \frac{1}{2} \left( \frac{\exp(\widehat{\mathbf{H}}_{ji})}{\sum_{k=1}^L \exp(\widehat{\mathbf{H}}_{jk})} + \frac{\exp(\widehat{\mathbf{H}}_{ji})}{\sum_{k=1}^L \exp(\widehat{\mathbf{H}}_{ki})} \right) \\
 &= \frac{1}{2} \left( \frac{\exp(\widehat{\mathbf{H}}_{ij})}{\sum_{k=1}^L \exp(\widehat{\mathbf{H}}_{kj})} + \frac{\exp(\widehat{\mathbf{H}}_{ij})}{\sum_{k=1}^L \exp(\widehat{\mathbf{H}}_{ik})} \right) \\
 &= \text{Row-Col-Softmax}(\widehat{\mathbf{H}}_{ij}).
 \end{aligned} \tag{18}$$

### B.2. Proof of Theorem 2

**Theorem 2.** Given a symmetric matrix  $\widehat{\mathbf{H}} \in \mathbb{R}^{L \times L}$ , the matrix Row-Col-Argmax( $\widehat{\mathbf{H}}$ ) is also a symmetric matrix.

*Proof:* From Eq. 11 and Eq. 12, we can know that:

$$\begin{aligned}
 & \text{Row-Col-Argmax}(\widehat{\mathbf{H}}_{ij}) = 1, \\
 & \text{if } \max\{\{\widehat{\mathbf{H}}_{ik}\}_{k=1}^L \cup \{\widehat{\mathbf{H}}_{kj}\}_{k=1}^L\} = \widehat{\mathbf{H}}_{ij},
 \end{aligned} \tag{19}$$

Table 8. Comparison between RNA secondary structure prediction methods and RFold.

Method	SPOT-RNA	E2Efold	UFold	RFold
constraint (a)	×	✓	✓	✓
constraint (b)	×	✓	✓	✓
constraint (c)	×	×	×	✓
sequence-to-map	pairwise concat	pairwise concat	hand-crafted	seq2map attention
F1 on RNAStralign test	0.711	0.686	0.915	<b>0.977</b>
Inference time on RNAStralign test	77.80 s	0.40 s	0.16 s	<b>0.02 s</b>

Then, we can infer that:

$$\begin{aligned} \text{Row-Col-Argmax}(\widehat{\mathbf{H}}_{ji}) &= 1, \\ \text{if } \max\{\{\widehat{\mathbf{H}}_{jk}\}_{k=1}^L \cup \{\widehat{\mathbf{H}}_{ki}\}_{k=1}^L\} &= \widehat{\mathbf{H}}_{ji}, \end{aligned} \quad (20)$$

As  $\widehat{\mathbf{H}}$  is a symmetric matrix,  $\widehat{\mathbf{H}}_{jk} = \widehat{\mathbf{H}}_{kj}$  and  $\widehat{\mathbf{H}}_{ki} = \widehat{\mathbf{H}}_{ik}$ . Thus, Row-Col-Argmax( $\widehat{\mathbf{H}}_{ji}$ ) can be rewritten as:

$$\begin{aligned} \text{Row-Col-Argmax}(\widehat{\mathbf{H}}_{ji}) &= 1, \\ \text{if } \max\{\{\widehat{\mathbf{H}}_{kj}\}_{k=1}^L \cup \{\widehat{\mathbf{H}}_{ik}\}_{k=1}^L\} &= \widehat{\mathbf{H}}_{ij}, \end{aligned} \quad (21)$$

It can be seen that only if  $\max\{\{\widehat{\mathbf{H}}_{kj}\}_{k=1}^L \cup \{\widehat{\mathbf{H}}_{ik}\}_{k=1}^L\} = \widehat{\mathbf{H}}_{ij} = \widehat{\mathbf{H}}_{ji}$ , then  $\widehat{\mathbf{H}}_{ij} = \widehat{\mathbf{H}}_{ji} = 1$ .

Thus, Row-Col-Argmax( $\widehat{\mathbf{H}}$ ) is also a symmetric matrix.

## C. Visualization

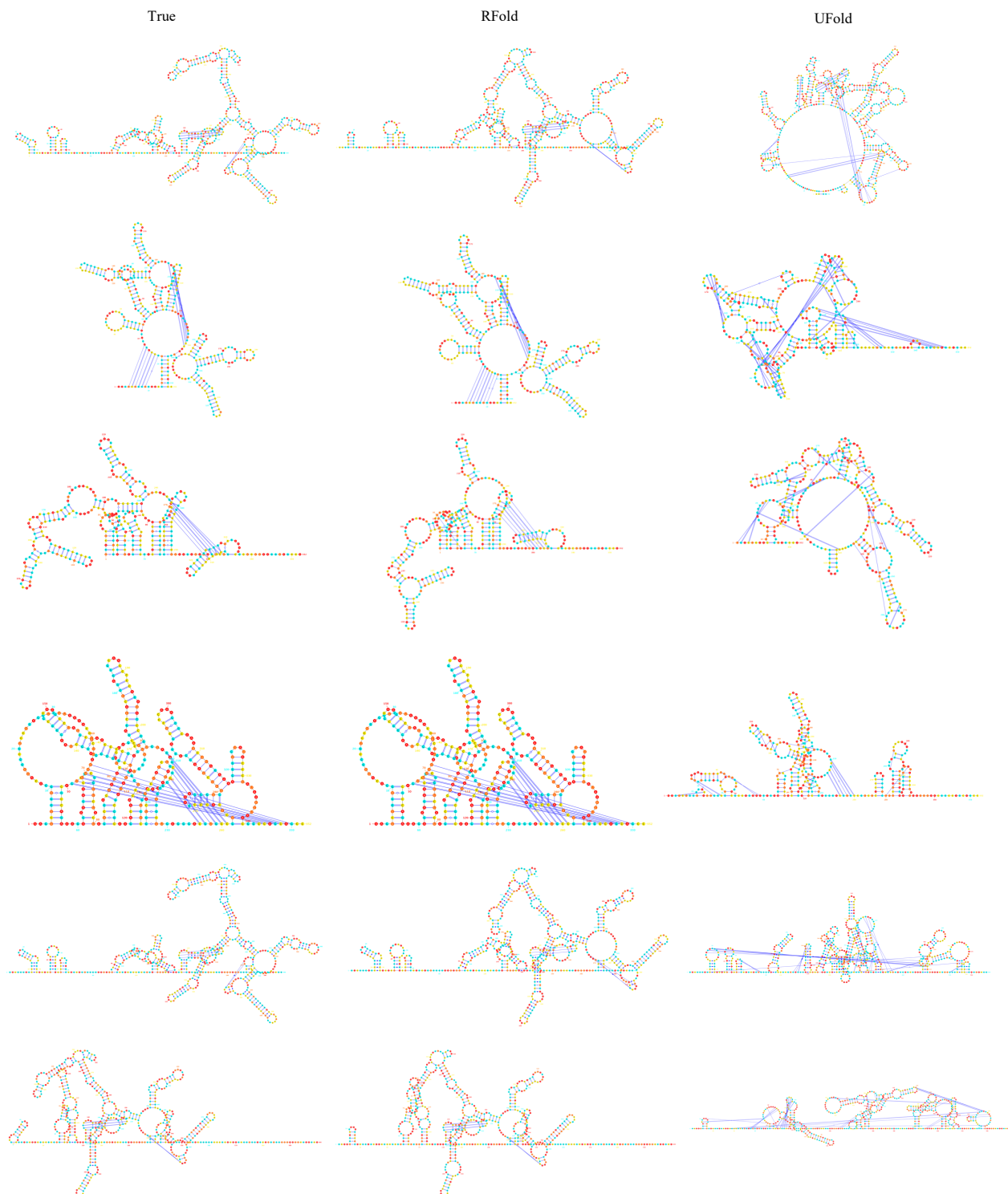


Figure 7. Visualization of the true and predicted structures.